

# We are IntechOpen, the world's leading publisher of Open Access books Built by scientists, for scientists

6,900

Open access books available

186,000

International authors and editors

200M

Downloads

Our authors are among the

154

Countries delivered to

TOP 1%

most cited scientists

12.2%

Contributors from top 500 universities



WEB OF SCIENCE™

Selection of our books indexed in the Book Citation Index  
in Web of Science™ Core Collection (BKCI)

Interested in publishing with us?  
Contact [book.department@intechopen.com](mailto:book.department@intechopen.com)

Numbers displayed above are based on latest data collected.  
For more information visit [www.intechopen.com](http://www.intechopen.com)



---

# Teaching Transmission Line Propagation and Plane Wave Reflection Using Software Tools

---

Susana Mota and Armando Rocha

Additional information is available at the end of the chapter

<http://dx.doi.org/10.5772/intechopen.74937>

---

## Abstract

Teaching transmission lines and wave propagation is a challenging task because it involves quantities not easily observable and also because the underlying mathematical equations—functions of time, distance and using complex numbers—are not prone to an easy physical interpretation in a frequent framework of a superposition of traveling waves in distinct directions. In such a context, tools with a strong visualization and easy student interaction can improve the learning outputs. We describe here a few tools and give basic exercises to address the main learning topics.

**Keywords:** telegrapher's equation, transmission line equations, input impedance, impedance matching, plane wave reflection and transmission

---

## 1. Introduction

The subject of propagation in transmission lines is a very important topic in analog microwave and high-speed digital circuits design. The full understanding of the circuit that models the transmission line, the line voltage and current equations, the input impedance of a transmission line and matching circuits is a basic background for any engineer dealing with circuits having sizes from an order of magnitude less than the wavelength. The wireless communications require a basic understanding of the multipath propagation channel whose basic models imply the understanding of plane wave reflection at the boundary between two infinite mediums. The phenomena described above are addressed here with very easy to use interactive tools developed in Matlab and that can assist teachers lecturing on these subjects and may also be used by the students as a virtual home laboratory. The first tools were already described in detail in [1] and made available and in <http://bit.ly/2m8oBoe>, whereas a new one

---

on plane waves that is available in <http://bit.ly/2m9TvMY> is now presented and comprehensively described here.

## 2. Transmission line model: TLM.m

An ideal transmission line is made of a pair of conductors that carries a signal along a path length  $\ell$  with only a delay  $\tau$ . Supposing a very high frequency and that any perturbation travels at finite speed we cannot assume that the voltage and current are constant along the line. Assuming two narrow parallel conducting strips of length  $\ell = 1$  m the image of a capacitor, with capacitance  $C_t(\text{F})$ , materializes immediately: an input voltage at one end will trigger a current to charge the capacitor. However, the two strips carrying the current can be seen also as a single rectangular turn of an inductor with inductance  $L_t(\text{H})$ : the current rate of change is limited. The equivalent circuit emerges as a series inductor followed by a capacitor to the ground.

This section addresses the response of a cascade of infinitesimal ladder circuits with length  $\Delta x$ , consisting of a series inductor with inductance  $L\Delta x$  and a capacitor to the GND with capacitance  $C\Delta x$ , where  $L$  (H/m) and  $C$  (F/m) are, respectively, a distributed inductance and a distributed capacitance.

### 2.1. The TLM script description and objectives

The TLM.m script analyses the frequency response of a chosen number of  $N$  cascaded cell circuits (i.e., a discretized transmission line) terminated by an arbitrary resistance  $R_L$ . The total inductance and capacitance correspond to that of a 1 m commercial coaxial cable with a characteristic impedance of  $Z_0 = 50 \Omega$ . The frequency response of the 1 m line is also calculated and depicted together with that of the discretized line, for comparison purposes.

The tool interface is shown in **Figure 1** depicting a simulation from DC to 1 GHz with 4 cells and  $Z_L = 50 \Omega$ . All the simulations are made assuming  $L = 189$  nH/m,  $C = 76$  pF/m and a generator with an internal impedance  $R_g = 50 \Omega$ . The main components of the tool and corresponding objectives are:

- Frame (1) shows the ladder circuit transfer function—the amplitude in dB (blue line) and the unwrapped phase in rad (green line)—and the transfer function of the ideal transmission line in the same format (black dotted line for the amplitude and red dotted line for the phase). The outputs intend to show that by increasing the number of cells the response of the discrete ladder circuit becomes close to that of the transmission line.
- Frame (2) shows the ladder circuit and the transmission line input resistance and input reactance using the same trace and color codes. The bottom slider is used to select a particular frequency and to highlight the ladder circuit response, in all the graphs, with a square marker. These values are also given in a table at the right of the slider. Additionally, the particular points of the frequency response can be examined.

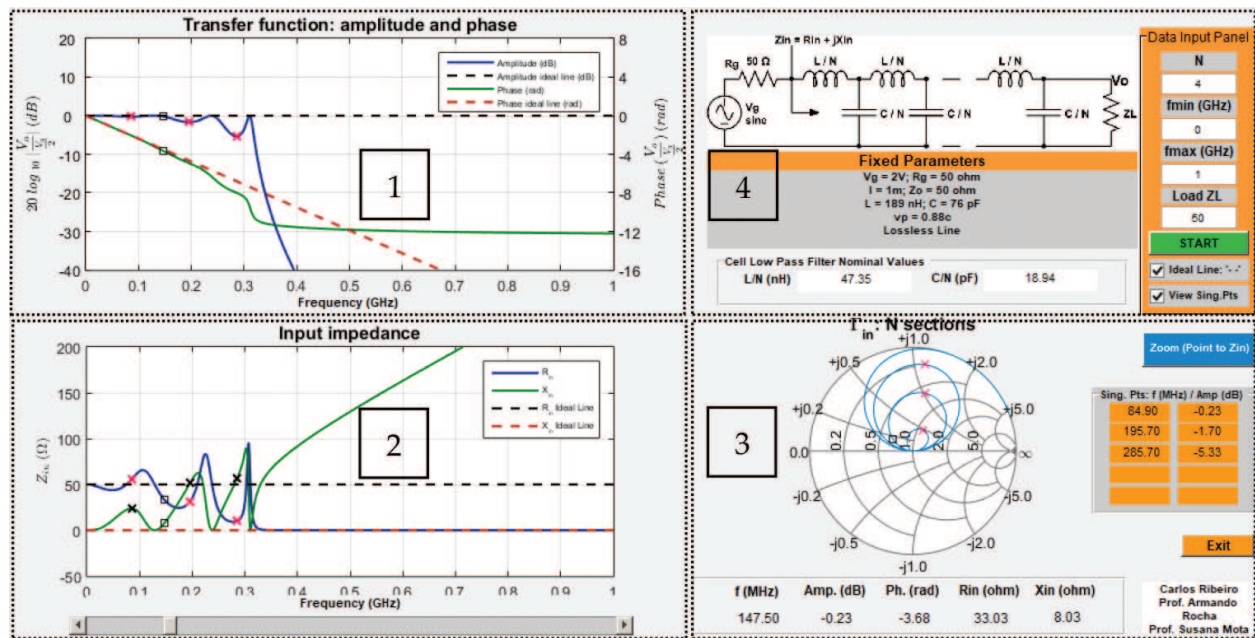


Figure 1. TLM Matlab tool aspect: frame description is given below.

- Frame (3) shows a Smith chart with the impedance of the ladder circuit and optionally, by activating an upper button, with the singular points at frequencies for which the transfer function is minimal. This output intends to show the trend of the discretized line input impedance in a Vector Network Analyzer (VNA) format.
- Frame (4) shows the schematics with the circuit parameters beneath. At the right, there is the input area allowing changing the simulation conditions (i.e., the frequency, number of cells and  $Z_L$ ).

## 2.2. A few exercises

Run the script with  $N = 1$  and the frequency range up to 1.5 GHz. Observe the results in **Figure 2** (left). Check if the single cell circuit is a low-pass filter whose impedance becomes purely reactive (inductive more specifically) and tends to an infinite value.

By increasing  $N = 5$  the filter bandwidth becomes larger and the impedance starts to exhibit a real part close to  $50 \Omega$  and an imaginary part still inductive, but, at some frequencies is null: resonances are occurring and the input impedance is  $Z_{in} = 50 \Omega$ . The response amplitude is 0 dB at these last frequencies with others exhibiting some local minima. The Smith chart and the numerical outputs allow the identification of these points easily. The trend of  $Z_{in}$  with frequency is an infinite inductive reactance: the first input cell dominates always the full circuit at a sufficiently high frequency that is related with  $N$ .

Increasing further the number of cells allows observing that the input resistance remains close to the  $50 \Omega$  and the input reactance remains close to  $0 \Omega$  for an increased bandwidth. Therefore, the circuit becomes an all pass filter with a delay, as can be observed from the linear phase exhibited by the frequency response of the circuit, approaching that of the ideal transmission line.

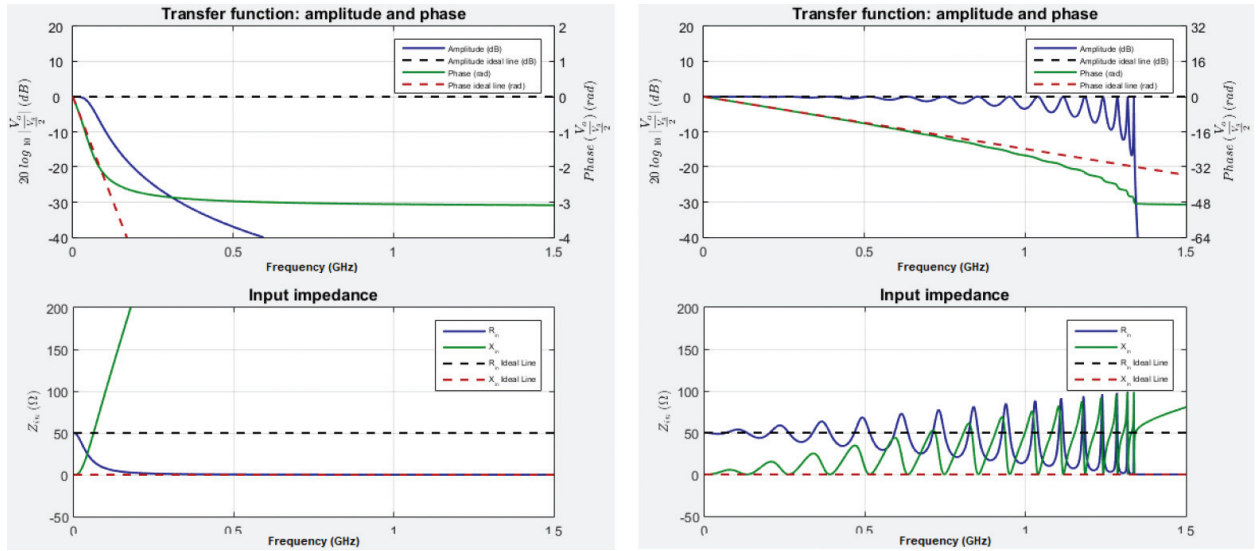


**Figure 2.** Transfer function and input impedance:  $N = 1$  (left) and  $N = 16$  (right).

### 2.3. Laboratory experiment

A laboratory prototype with  $N = 6$  sections was implemented as can be observed in **Figure 3(a)**. The ladder circuit uses inductors with an average  $L_1 = 36.7$  nH and capacitors with an average  $C_1 = 16.0$  pF, ( $\sqrt{LC^{-1}} \cong 50\Omega$ ). Furthermore, a lumped low-pass L-C circuit, with the integrated

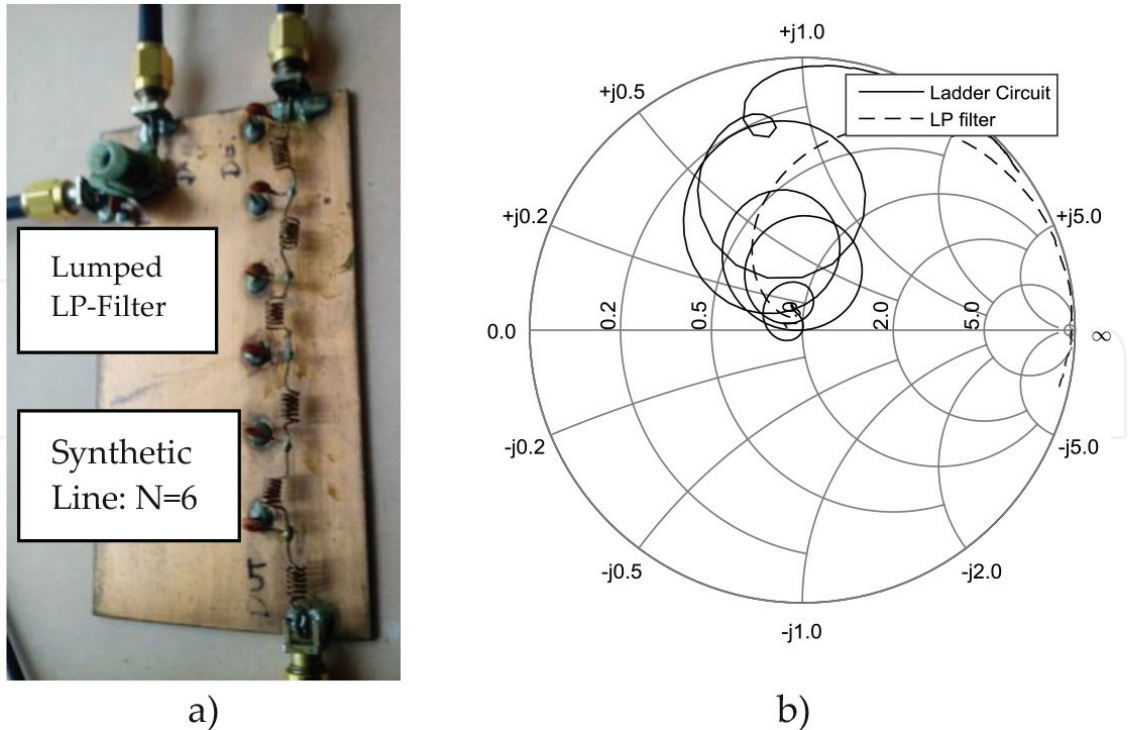


**Figure 3.** (a) Synthetic line with  $N = 6$  and a lumped low-pass L-C circuit; (b)  $Z_{in}$  measured with a VNA up to 400 MHz.



inductance and capacitance of the ladder circuit elements, was added to the PCB for comparison purposes. The impedance of both circuits was measured with a VNA and is presented in **Figure 3(b)**.

As can be observed, the ladder circuit impedance follows in major lines the expected behavior, including the trend with the frequency to become a very high inductive impedance, in spite of some noticeable deviation at higher frequencies and not the perfect “ties” in general. The global similarity can be tested with TLM.m simulations using  $N = 6$ . On the other hand, the LP filter shows the expected trend: the input impedance becomes a very high inductive value at an early frequency if compared to the ladder circuit. In fact, the impedance even becomes capacitive: the anomaly is due to the non-ideality of the components, namely the serial resonance of the inductor.

In spite of the non-ideality of the frequency response of the components and other implementation difficulties, the prototype is very promising as a pedagogical tool to teach the circuit model of transmission line: it represents the telegrapher’s equation physical model. Eventually, having a single L-C circuit, a circuit with  $N = 2$  and another one with  $N = 4$  may be recommended. The hardware implementation requires the use of high quality inductors and capacitors (high self-resonance frequency: small nominal values are recommended), equalization of the nominal values and a careful layout of the inductors to minimize mutual inductance.

Another interesting and easy exercise for the student is to compute, himself, the input impedance of the circuit with  $N$  cascaded cells, by using the recursive equation:

$$Z_n = j\omega L_1 + \frac{Z_{n-1}}{1 + jZ_{n-1}\omega C_1} \quad (1)$$

where  $n$  goes from 1 to  $N$  and the starting condition is  $Z_{n-1} = Z_L$ , for  $n = 1$ . With a little effort Eq. (1) can be implemented and computed in Matlab for any range of frequencies, an arbitrary number  $N$  of sections or even load impedances (other details, such as how to compute the transfer function, can be found in [1]).

### 3. Transmission line input impedance: Zin.m

Wave propagation—voltage and current—in transmission lines is usually handled by employing phasor analysis. In this context, it is crucial to understand that, in general, there are two waves traveling in opposite directions and that their relative phase changes along the line. Consequently, a standing wave is produced for voltage and current. The Zin tool explores the characteristics of the line input impedance by displaying simultaneously the amplitudes of the voltage and current standing waves and the corresponding phasors. Therefore, the relative amplitude and phase between them may be associated with the standing waves. The input impedance may be observed at any arbitrary point in a line of one-wavelength long, enabling this way, the perception of the impedance periodic behavior for lossless lines.

### 3.1. Description and objectives

The application assumes a transmission line with  $Z_0 = 50 \Omega$  and a generator with an amplitude of 2 V and internal impedance of  $50 \Omega$ . The tool interface is depicted in **Figure 4** and its description is as follows:

- On the top, it is shown the line circuit schematic, and on its right, there is a small area for entering the simulation parameters: the load impedance and the attenuation coefficient may be introduced. Above the schematic, there is an *information area* for results output, displaying the VSWR, the maximum and the minimum values of the resistance and reactance along the line. These results are updated every time any input is changed.
- Below the schematic, there is a rectangular graph where the normalized voltage phasor,  $1+\Gamma(d)$ , and the normalized current phasor,  $1-\Gamma(d)$ , are represented (in blue and red, respectively) at one point  $d$  of the line, which is chosen by actuating on the slider below this diagram. Furthermore, the voltage and current amplitudes along the line are also shown. Closely, on the right of this graph there is a new area for results output, presenting the reflection coefficient in the chosen point of the line, using rectangular and polar coordinates. At the rightmost side, the reflection coefficient, along the line, is also presented graphically in polar coordinates.
- At the bottom left, there is another rectangular graph exhibiting the observed resistance and reactance along the line (in blue and red, respectively). In addition, at the bottom rightmost side, the impedance along the line is represented again, this time in the complex plane. Below this representation, there is one more area for results output displaying the resistance and reactance at the selected line point.

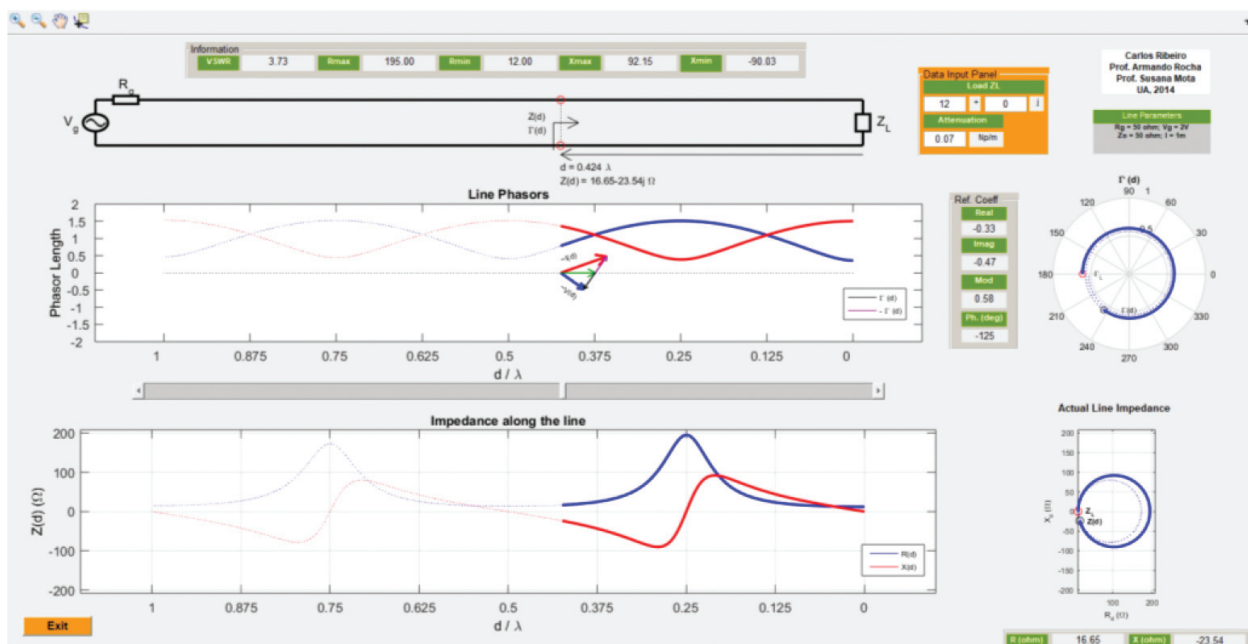


Figure 4. The interface of the input impedance demonstrator.

The picture of the reflection coefficient in a polar representation, as it is usually measured in laboratory using VNAs, intends to introduce or reinforce, in a straightforward way, the “Towards generator” or “Towards load” concepts, facilitating the understanding and use of the Smith chart. The impedance graph aims to establish the relationship between the type of impedance (with inductive or capacitive reactance) and the quadrant where the complex coefficient is represented and to establish also that the reflection coefficient and the corresponding impedance both describe a circumference (i.e., there is a conformal transformation between both).

### 3.2. A few exercises

Consider the lossless line with a resistive load impedance being two to five times smaller (or larger) than the characteristic impedance, for example, as  $12\ \Omega$ .

- Observe the fluctuations on the voltage and current amplitudes along the line, the resulting input impedance, by inspecting both representations (the rectangular and complex plane graphs) and the reflection coefficient. Notice that the impedance at  $d = 0.25\lambda$  is again purely resistive (but greater than the characteristic impedance), whereas at  $d = 0.5\lambda$  it is exactly equal to the load impedance again.
- Also, analyze the behavior of the input impedance at the standing wave maxima and minima points, and notice that the impedance nature (capacitive/inductive) changes, that is, at these points, the line behaves as a resonant circuit. Try to identify the type of resonance (series/parallel) exhibited at each of these points. Hint: consider a small increase/reduction in the frequency (i.e., a small reduction/increase of the wavelength) and compare with the lumped resonant circuits.
- Within the first line section of  $0.5\lambda$  length, closer to the load, locate two points where the resistance of the observed impedance is equal to the line characteristic impedance and annotate the corresponding reactance. Explain how this reactance could be canceled by using, for example, a lumped element.

Maintaining the lossless line, study other loads as the *short-circuit* (SC), *open-circuit* (OC) and purely reactive impedances. In addition to  $d = 0.25\lambda$  and  $d = 0.5\lambda$ , considered previously, also observe the line impedance at  $d = 0.125\lambda$ .

Consider now a lossy line and repeat the simulations with the loads suggested in the previous paragraphs. The results presented in **Figure 4** refer to a  $12\ \Omega$  load and those in **Figure 5** refer to the SC. In both cases, it was considered a transmission line with an attenuation coefficient of  $0.07\ \text{Np/m}$ . Notice that voltage and current phase relations are maintained, but their amplitude fluctuations are more significant near the load. On the other hand, near the line input (generator) these fluctuations tend to vanish, particularly for highly attenuating lines (to better observe this effect, it is advisable to increase the attenuation coefficient). As a result, both the reflection coefficient and the input line impedance trace a spiral converging to the line characteristic impedance.



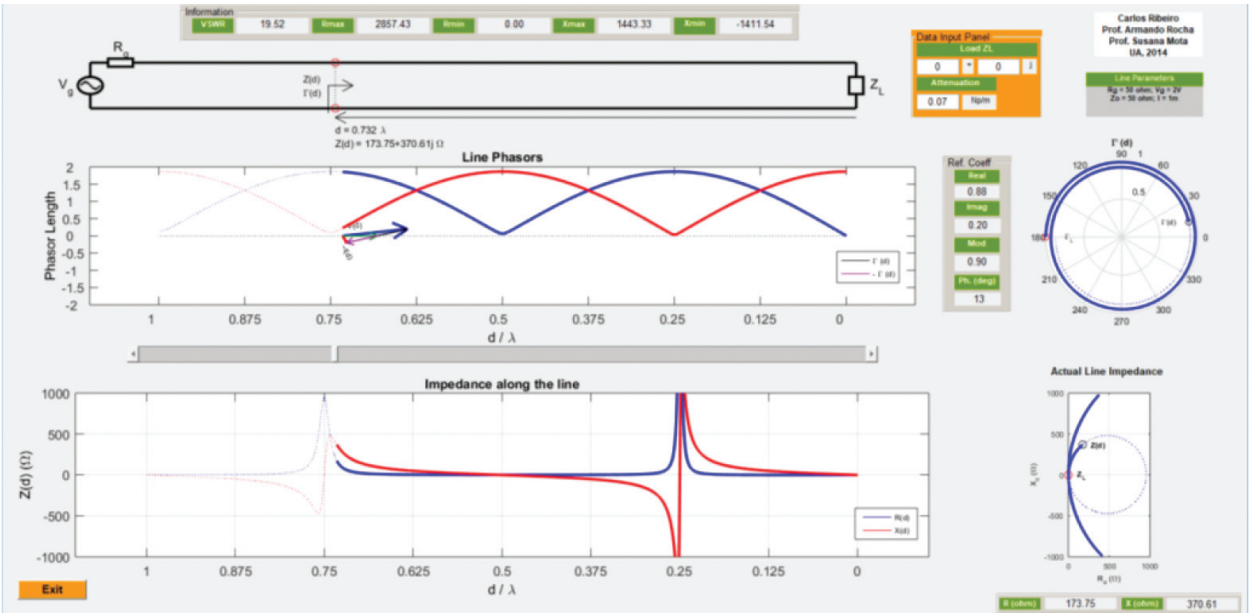


Figure 5. Input impedance of a lossy transmission line terminated in SC.

3.3. Laboratory experiment

Figure 6 displays experimental results obtained for a microstrip line terminated in SC whose length is 6.2 cm, which equals one wavelength at about 2.73 GHz.

The reflection coefficient, presented in Figure 6(b), was measured using a VNA, from 500 kHz (almost DC) up to 2 GHz. This line may be considered as a practical implementation for the input parameters used in Figure 5, even though, the measurements were acquired in the frequency domain, not along the line as shown by the demonstrator. In fact, it is possible to

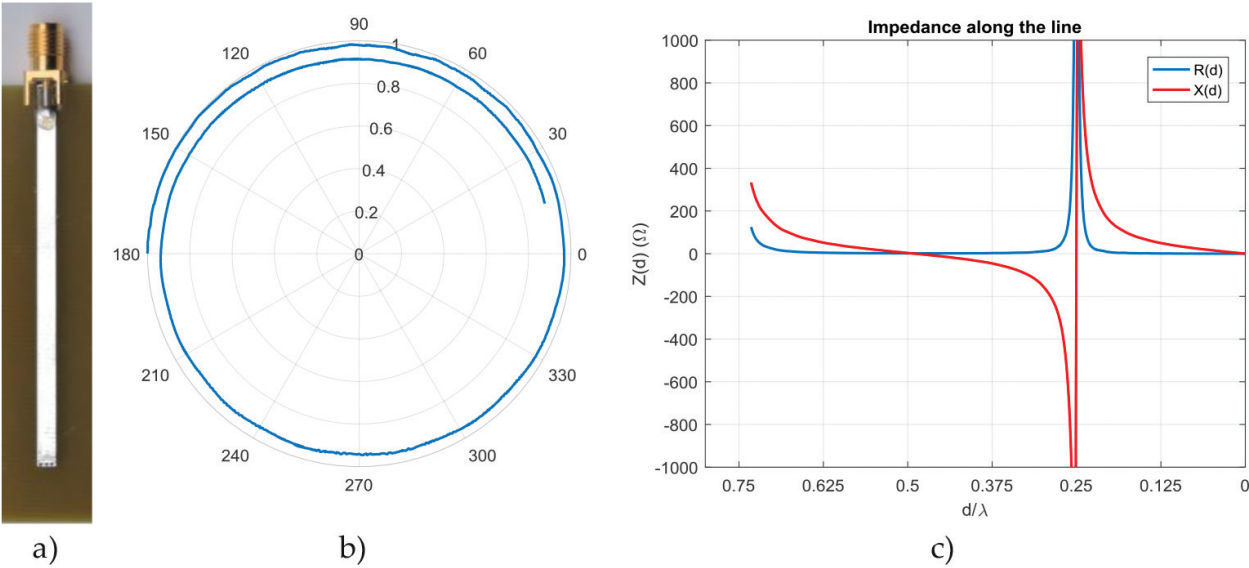
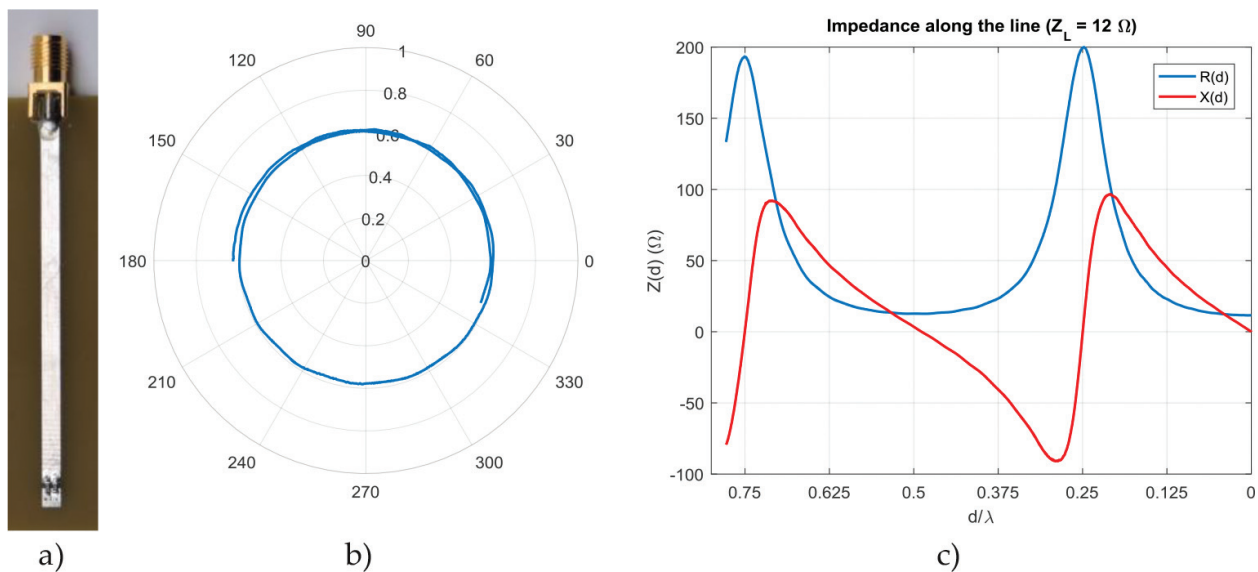


Figure 6. (a) Microstrip line terminated in SC; (b) the input reflection coefficient measured from 500 kHz up to 2 GHz; and (c) the corresponding input impedance.



**Figure 7.** (a) Microstrip line terminated with  $Z_L = 12 \Omega$ ; (b) the input reflection coefficient measured from 500 kHz up to 2 GHz; and (c) the corresponding input impedance.

achieve quite consistent results, because, the demonstrator considers an increasing distance to the load, while, the measurements include an increasing attenuation coefficient with frequency for a constant line length.

The resistance and reactance of the impedance along the line are also presented in **Figure 6(c)**. In order to make the comparison with the results from the demonstrator easier (**Figure 5**), the frequency axis has been translated into electrical distance by using the frequency for which the line length equals one wavelength.

**Figure 7** displays the same type of experimental results obtained for a microstrip line with the same physical properties and terminated with  $Z_L = 12 \Omega$ . This line may be viewed as a practical implementation for the input parameters used in **Figure 4**. In this case, similarly to the line-terminated SC, the reflection coefficient starts with an angle of  $180^\circ$  and its angular excursion should be the same, since the physical properties of the two lines are identical. However, the reflection coefficient in **Figure 7(b)** presents a larger angular excursion, suggesting a longer line or, in alternative, a load with a small inductive element. In fact, this can be due to the small patch used for welding the load to the ground plane below the substrate or the non-ideality of the resistor. Therefore, the frequency for which the line length appears to be one wavelength decreased to 2.57 GHz, which is about 6% less than that of the SC. Consequently, by using this value to obtain the electrical distance, for the abscissa axis in **Figure 7(c)**, results in an apparently longer transmission line.

#### 4. Impedance matching: Matching.m

This application helps to find a matching solution expending a single series or parallel element. The solution is not given immediately; instead, it is intended to be found by experimentation,

using the properties of the transmission line impedance, that is, the user must find an appropriate distance to the load where to insert a susceptance (parallel) or a reactance (series) and the corresponding length (for a stub) or the nominal component value (if a lumped element is used).

The demonstrator shows the transmission line together with the stub or the lumped component, and uses the Smith chart so that the user is able to evaluate the outcome of all the inputs or changes introduced, by displaying the input impedance or admittance on the Smith chart and also, numerically, next to the circuit schematic. Furthermore, assuming that the reactance of the load does not change with frequency, the circuit frequency response is presented on the Smith chart and, in addition, on one rectangular graph window (return loss, VSWR or transmission loss can be represented).

#### 4.1. Description and objectives

The tool assumes a generator with internal impedance of  $50\ \Omega$  and a lossless transmission line with characteristic impedance of  $50\ \Omega$ , with a length that is  $0.5\lambda$  at the chosen frequency. The user interface is depicted in **Figure 8** and its description is as follows:

- On the upper left side it is shown the circuit schematic and, on its right there is an area for entering the parameters, where the user can specify the load impedance, the project frequency ( $f_p$ ), the type of matching network (series or parallel) and the type of the matching element (inductor, capacitor or OC/SC terminated stub). Any of these options may be set and changed at any time by the user.
- Below the circuit schematic, there is a slider allowing the user to choose where to place the matching component and, below the slider, a Smith chart is displayed. As the slider is moved, the line impedance for series arrangements (or admittance for parallel arrangements) is displayed on the Smith chart using a blue line. Simultaneously, the corresponding numerical values are given next to the slider.
- The matching element (stub or lumped component) may be adjusted using another slider inside the area for parameter inputs. The resulting impedance (or admittance) is immediately shown on the Smith chart using a green line. At the same time, numerical values are also displayed near this slider: stub length (or nominal value of the lumped component), corresponding reactance (or susceptance in absolute value), position of the matching network, and the VSWR achieved.
- At the bottom right side, a rectangular window presents the return loss, transmission loss or the VSWR: the user can choose one of the three which is displayed as a function of the frequency from  $f_p/2$  to  $10f_p$ . In addition, a “check box” allows, at any moment, to visualize also the impedance frequency response on the Smith chart (or remove it).

#### 4.2. A few exercises

Consider  $Z_L = 12\ \Omega$  and  $f_p = 700\ \text{MHz}$ . Start by introducing a series network using a lumped component:

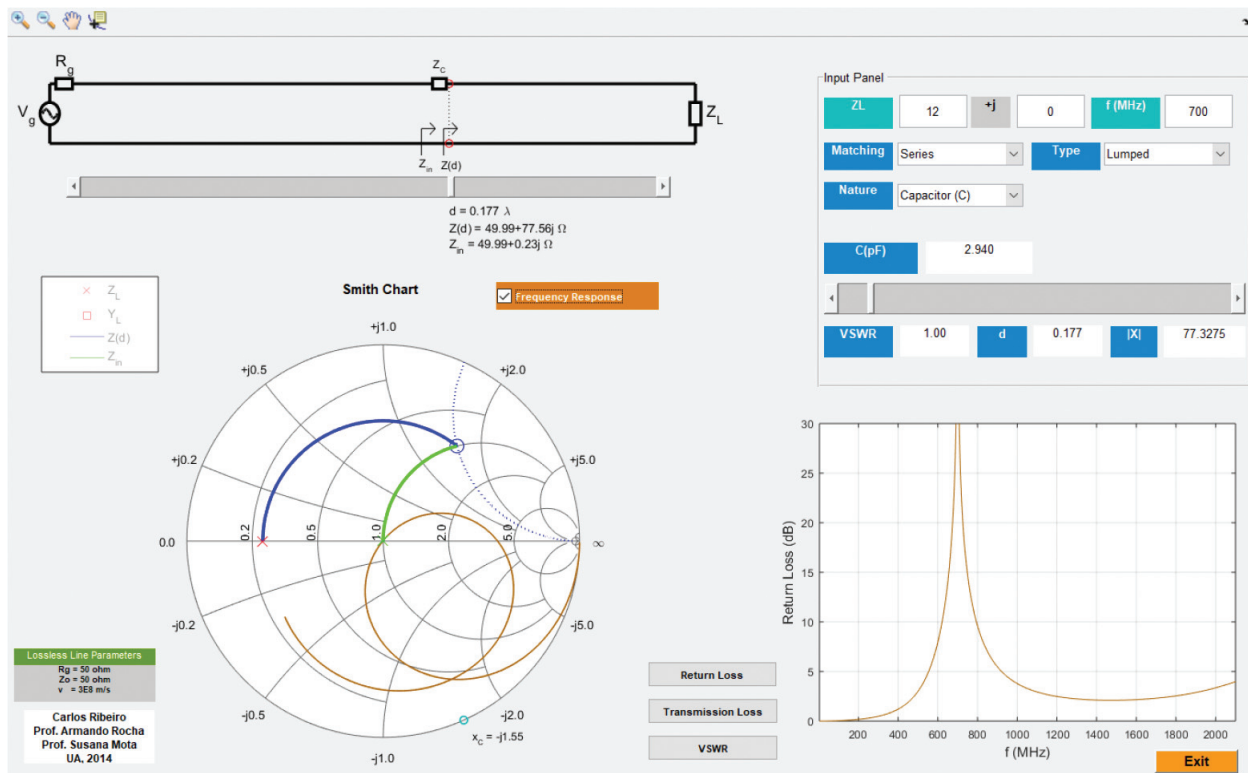


Figure 8. The interface of the matching demonstrator.

- By actuating in the slider below the circuit schematic locate the first point in line (as close to the load as possible) where the real part of  $Z(d)$  is about  $50 \Omega$ . Then move the other slider inside the parameter input panel and try to reach the center of the Smith chart. This is the solution depicted in **Figure 8**. Confirm that only one of the available components (inductor or capacitor) allows matching the transmission line.
- Locate a second point in the line where the real part of  $Z(d)$  is again  $50 \Omega$ , and find the lumped component which matches the system. Verify whether there is an alternative position on the line (different from those found previously) where a match can be achieved. Observe the input impedance, the VSWR and the return loss as a function of the frequency. Try to explain the behavior of the return loss when the frequency tends to infinity.
- Summarize all solutions found: two possible points per half wavelength to insert the component and, that for each position, only one type of lumped component (inductor or capacitor) offers a solution to the problem.

Consider now  $Z_L = 12.5 \Omega$ ,  $f_p = 650$  MHz and achieve the matching using a parallel stub:

- Move the slider below the schematic and find one first position on the line (as close to the load as possible) where the real part of  $Y(d)$  is about  $1/50$  S and notice that at this location, the equivalent impedance,  $Z_{inv}$  involves a  $50 \Omega$  resistor in parallel with a certain reactance. Then, move the slider inside the parameter input panel and try to reach the center of the

Smith chart. Annotate the corresponding stub lengths for OC and SC terminations. **Figure 9** presents the solution using a stub in OC.

- Observe that, at certain frequency, the return loss reaches the worst value of 0 dB (meaning that the reflection coefficient touches somewhere the outer circle of the Smith chart, that is,  $|\Gamma| = 1$ ). Try to explain this observation.
- Repeat this last exercise using lumped elements and notice that for each of the above positions (those where it is possible to match the line impedance with parallel stubs) there is only one lumped element that allows to match the line.

4.3. Laboratory experiment

**Figure 10(a)** shows a practical implementation of the solution given in **Figure 8**. Its input impedance was measured, from 500 kHz up to 2 GHz, using a VNA and is represented in **Figure 10(b)**. The corresponding return loss is presented in **Figure 10(c)**. The best return loss value (highlighted by an asterisk in the figure) is slightly better than 15 dB and it is achieved at nearly the project frequency (698 MHz).

Furthermore, **Figure 11(a)** depicts a practical implementation of the solution found in **Figure 9**. In the same way, **Figure 11(b)** and **(c)** show, respectively, the measured input impedance and the corresponding return loss. At the project frequency (650 MHz) the return loss measured is about 20.4 dB (the best return loss value is about 21 dB achieved at 637 MHz).

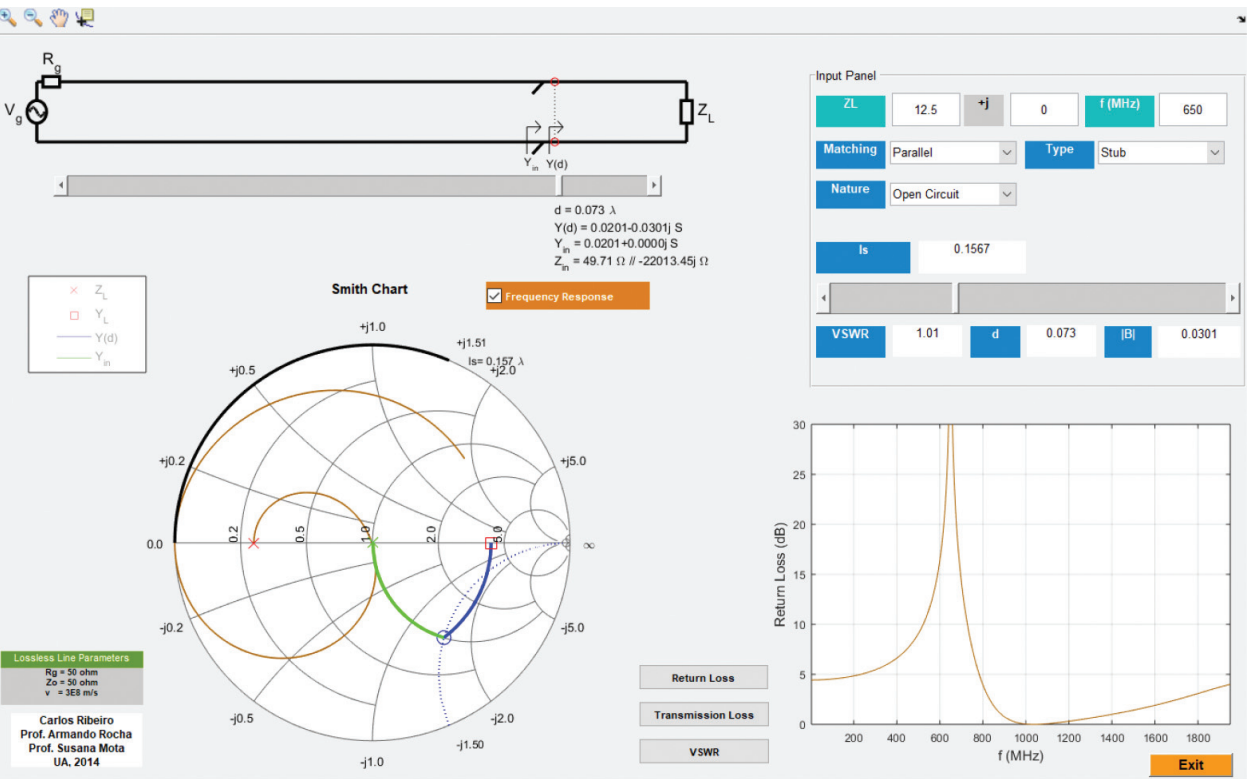


**Figure 9.** Matching  $Z_L = 12.5 \Omega$  at  $f_p = 650 \text{ MHz}$  with a parallel stub in OC.



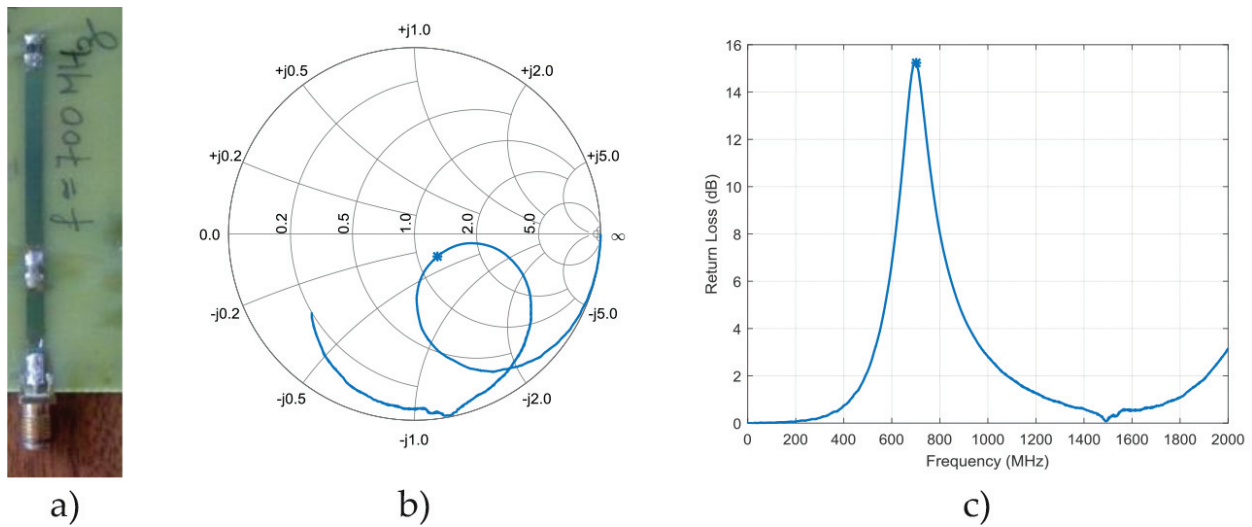


**Figure 10.** (a) Matching  $Z_L = 12 \Omega$  at  $f_p = 700 \text{ MHz}$  using a series capacitor, (b) the measured input impedance, and (c) measured return loss.

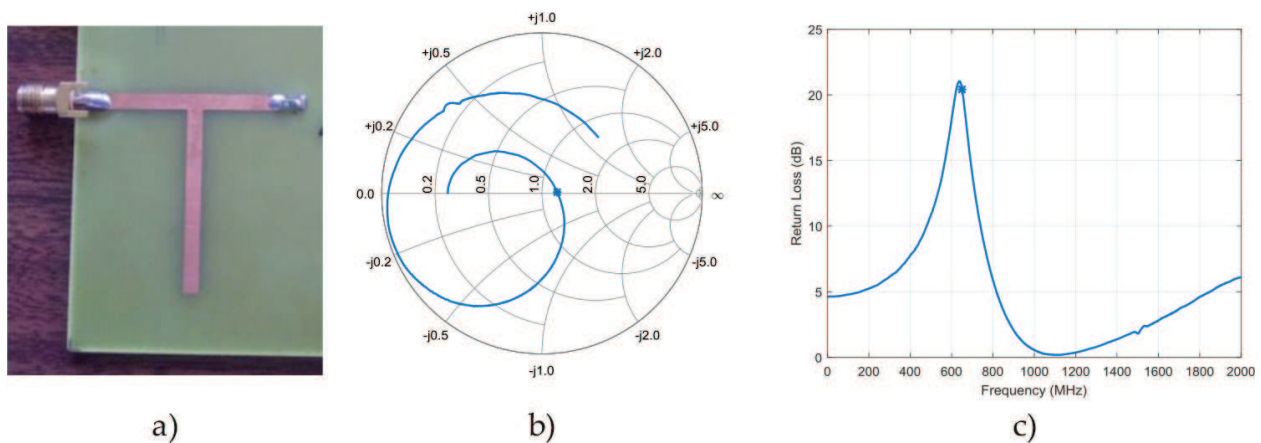


**Figure 11.** (a) Matching  $Z_L = 12.5 \Omega$  at  $f_p = 650 \text{ MHz}$ , with a parallel OC stub, (b) the measured input impedance, and (c) measured return loss.

In both cases, the results displayed by the demonstrator are generally in good agreement with those from the measurements.

## 5. Electromagnetic waves: EM.m

The reflection and transmission of electromagnetic plane waves is a fundamental resource to understand wireless multipath propagation channel models and to introduce basic concepts concerning propagation phenomena in optical fibers. Teaching this matter is even more difficult than the transmission lines one. To justify we can point out the following reasons: the phenomenon depends on the wave polarization; vectors should be used to represent electromagnetic fields (3-D visualization or similar is mandatory); the superposition of incident and

reflected fields is more complex, because, waves do not travel in the same direction; and finally, there are particular cases, such as, the total transmission (Brewster angle) and the total reflection (above a critical angle), of incident plane waves.

### 5.1. The EM.m script description and objectives

Let us assume an electromagnetic plane wave traveling in a medium 1 impinging on a plane infinite boundary (from now on called *reflection plane*) between two lossless mediums: medium 1 and medium 2, having, respectively, a dielectric permittivity  $\epsilon_1$  and  $\epsilon_2$ . Both mediums are non-magnetic, that is,  $\mu_1 = \mu_2 = \mu_0$ , with  $\mu_0$  being the vacuum permeability. The dielectric permittivity,  $\epsilon$ , can be written using the relative permittivity,  $\epsilon_r$ , as  $\epsilon = \epsilon_r \epsilon_0$ , with  $\epsilon_0$  being the free space permittivity.

The impedance of a medium is given by.

$$\eta = \frac{120\pi}{\sqrt{\epsilon_r}} \quad (\Omega) \quad (2)$$

and the wavenumber (or phase constant) is given by:

$$\beta = \frac{2\pi\sqrt{\epsilon_r}}{\lambda_0} \quad (\text{rad/m}) \quad (3)$$

with  $\lambda_0$  being the free space wavelength. The *angle of incidence*,  $\theta_i$ , is defined as the angle between the direction of propagation,  $\hat{k}_i$ , and the normal to the reflection plane (please see **Figure 12**). The *incidence plane* is the plane defined by the direction of propagation and the normal to the reflection plane (XoZ plane). The incident wave causes a reflected wave, having an angle of reflection equal to the angle of incidence, and a transmitted wave propagating on medium 2, having an angle of transmission,  $\theta_t$ , given by:

$$\sin \theta_t = \sqrt{\frac{\epsilon_{r1}}{\epsilon_{r2}}} \sin \theta_i \quad (4)$$

Two distinct linearly polarized incident plane waves, **Figure 12**, can be identified:

- A polarization with the electric field parallel to the incidence plane,  $E_{\parallel}$ , having components along z and x. The orthogonal magnetic field,  $H_{\parallel}$ , has a component along y.
- A polarization with the electric field perpendicular to the incidence plane,  $E_{\perp}$ . The orthogonal magnetic field,  $H_{\perp}$ , has components along z and x.

The reflection coefficient,  $\Gamma$ , and the transmission coefficient,  $T$ , for the parallel polarization, are given by:

$$\Gamma_{\parallel} = \frac{\sqrt{\left(1 - \frac{\epsilon_{r1}}{\epsilon_{r2}} \sin^2 \theta_i\right)} - \sqrt{\frac{\epsilon_{r2}}{\epsilon_{r1}}} \cos \theta_i}{\sqrt{\left(1 - \frac{\epsilon_{r1}}{\epsilon_{r2}} \sin^2 \theta_i\right)} + \sqrt{\frac{\epsilon_{r2}}{\epsilon_{r1}}} \cos \theta_i} \quad T_{\parallel} = (1 + \Gamma_{\parallel}) \frac{\cos \theta_i}{\cos \theta_t} \quad (5)$$

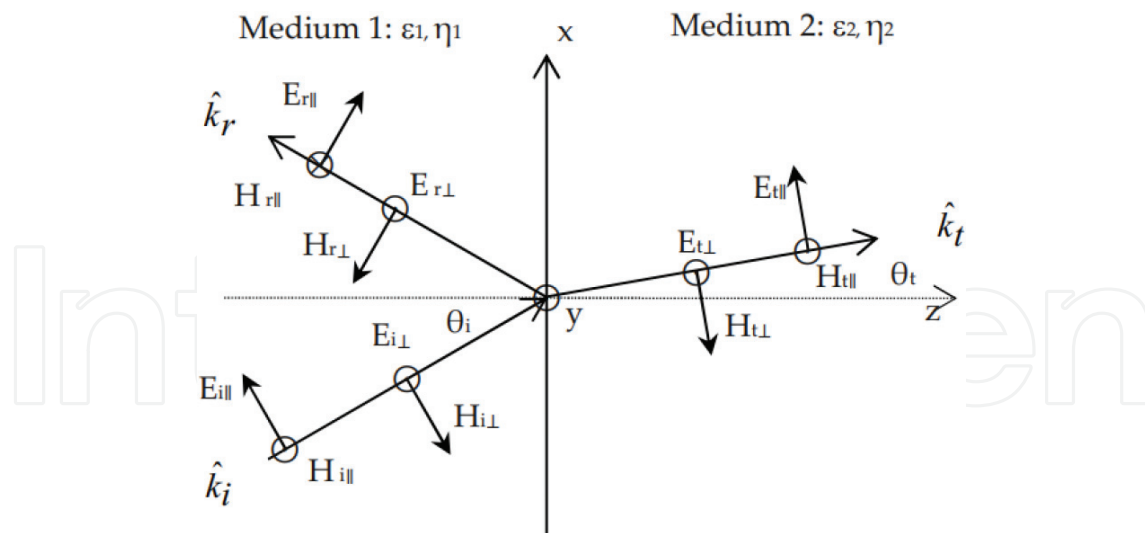


**Figure 12.** Plane wave incidence (plane XoY): ‘i’, ‘r’ and ‘t’ means incident, reflected and transmitted waves, the unit vector along the incident, reflected and transmitted waves direction of propagation are  $\hat{k}_i, \hat{k}_r, \hat{k}_t$ , the symbol  $\odot$  means vector pointing to the reader and  $\otimes$  pointing downwards.

with  $\theta_t$  given by Eq. (4) and, for the perpendicular polarization, are given by:

$$\Gamma_{\perp} = \frac{\cos \theta_i - \sqrt{\frac{\epsilon_{r2}}{\epsilon_{r1}} - \sin^2 \theta_i}}{\cos \theta_i + \sqrt{\frac{\epsilon_{r2}}{\epsilon_{r1}} - \sin^2 \theta_i}} \quad T_{\perp} = 1 + \Gamma_{\perp} \quad (6)$$

It can be shown that, for parallel polarization, there is an angle of incidence,  $\theta_{iB}$ , called *Brewster angle* at which the reflection coefficient becomes null. This angle is given by:

$$\theta_{iB} = \sin^{-1} \sqrt{\frac{\epsilon_{r2}}{\epsilon_{r1} + \epsilon_{r2}}} \quad (7)$$

In addition, regardless the wave polarization there is an angle of incidence, for the case of incidence in a less dense medium, which turns the absolute value of the reflection coefficient unitary. This is the *critical angle*,  $\theta_{ic}$ , given by:

$$\theta_{ic} = \sin^{-1} \left( \sqrt{\frac{\epsilon_{r2}}{\epsilon_{r1}}} \right) \quad (8)$$

For the parallel polarization, the following set of electric and magnetic fields equations can be derived using Eqs. (2)–(5):

$$\vec{E}_i(x, z) = E_{io}(\hat{x} \cos \theta_i - \hat{z} \sin \theta_i) e^{-j\beta_1(x \sin \theta_i + z \cos \theta_i)} \quad (9)$$

$$\vec{H}_i(x, z) = \hat{y} \frac{E_{io}}{\eta_1} e^{-j\beta_1(x \sin \theta_i + z \cos \theta_i)} \quad (10)$$

$$\vec{E}_r(x, z) = \Gamma_{\parallel} E_{io}(\hat{x} \cos \theta_i + \hat{z} \sin \theta_i) e^{-j\beta_1(x \sin \theta_i - z \cos \theta_i)} \quad (11)$$

$$\vec{\mathbf{H}}_r(x, z) = -\hat{y} \Gamma_{\parallel} \frac{\mathbf{E}_{io}}{\eta_1} e^{-j\beta_1 (x \sin \theta_r - z \cos \theta_r)} \quad (12)$$

$$\vec{\mathbf{E}}_t(x, z) = T_{\parallel} \mathbf{E}_{io} (\hat{x} \cos \theta_t - \hat{z} \sin \theta_t) e^{-j\beta_2 (x \sin \theta_t + z \cos \theta_t)} \quad (13)$$

$$\vec{\mathbf{H}}_t(x, z) = \hat{y} T_{\parallel} \frac{\mathbf{E}_{io}}{\eta_2} e^{-j\beta_2 (x \sin \theta_t + z \cos \theta_t)} \quad (14)$$

with  $\mathbf{E}_{io}$  being a reference incident electric field amplitude.

Similarly, using Eqs. (2)–(4) and (6) the following equations can be derived for the perpendicular polarization:

$$\vec{\mathbf{E}}_i(x, z) = \hat{y} \mathbf{E}_{io} e^{-j\beta_1 (x \sin \theta_i + z \cos \theta_i)} \quad (15)$$

$$\vec{\mathbf{H}}_i(x, z) = \frac{\mathbf{E}_{io}}{\eta_1} (-\hat{x} \cos \theta_i + \hat{z} \sin \theta_i) e^{-j\beta_1 (x \sin \theta_i + z \cos \theta_i)} \quad (16)$$

$$\vec{\mathbf{E}}_r(x, z) = \hat{y} \Gamma_{\perp} \mathbf{E}_{io} e^{-j\beta_1 (x \sin \theta_i - z \cos \theta_i)} \quad (17)$$

$$\vec{\mathbf{H}}_r(x, z) = \frac{\Gamma_{\perp} \mathbf{E}_{io}}{\eta_1} (\hat{x} \cos \theta_i + \hat{z} \sin \theta_i) e^{-j\beta_1 (x \sin \theta_i - z \cos \theta_i)} \quad (18)$$

$$\vec{\mathbf{E}}_t(x, z) = \hat{y} T_{\perp} \mathbf{E}_{io} e^{-j\beta_2 (x \sin \theta_t + z \cos \theta_t)} \quad (19)$$

$$\vec{\mathbf{H}}_t(x, z) = \frac{T_{\perp} \mathbf{E}_{io}}{\eta_2} (-\hat{x} \cos \theta_t + \hat{z} \sin \theta_t) e^{-j\beta_2 (x \sin \theta_t + z \cos \theta_t)} \quad (20)$$

The interpretation of Eqs. (5) and (6) and the fields given from Eqs. (9)–(20) as a function of  $\theta_i$  is difficult. The EM.m script addresses this problem by depicting the reflection coefficients and all the set of fields in three separate figures. A screenshot of the tool interface, that follows a similar but more complete approach of the one described in [2], is presented in **Figure 13**.

The interface is divided in four graphs (left part) and an input data/output area (right part). The numbered areas contain:

1. The fields with a single Cartesian component along  $\hat{y}$ :  $E_{i\perp}$ ,  $E_{r\perp}$ , or the total field  $E_{1\perp} = E_{i\perp} + E_{r\perp}$  in medium 1 and  $E_{t\perp}$  in medium 2 for the perpendicular polarization;  $H_{i\parallel}$ ,  $H_{r\parallel}$ , or the total field  $H_{1\parallel} = H_{i\parallel} + H_{r\parallel}$  in medium 1 and  $H_{t\parallel}$  in medium 2 for the parallel polarization. The representation contains also the directions of the incident, reflected and transmitted waves (represented by segments as in **Figure 12**) and the wavelength in medium 1 and 2 and along the  $\hat{x}$  and  $\hat{z}$  axis (written equations).
2. The fields along the  $\hat{z}$  axis:  $H_{iz\perp}$ ,  $H_{rz\perp}$ , or the total field  $H_{tz\perp} = H_{iz\perp} + H_{rz\perp}$  in medium 1 and  $E_{tz\perp}$  in medium 2 for the perpendicular polarization;  $E_{iz\parallel}$ ,  $E_{rz\parallel}$ , or the total field  $E_{1\parallel} = E_{iz\parallel} + E_{rz\parallel}$  in medium 1 and  $E_{tz\parallel}$  in medium 2 for the parallel polarization.
3. The fields along the  $\hat{x}$  axis (as described above).

4. The amplitude of the reflection and transmission coefficients and their respective phase. The slider can be used to change the angle of incidence.
5. The interaction tools to choose the incident polarization, the angle of incidence, the dielectric constants, the angle of incidence and the waves to be displayed (i, r or t).
6. The numerical outputs: reflection and transmission coefficients, angle of transmission and the critical or Brewster angle (if they exist).

The simulations are made for a normalized electric field amplitude of 1 V/m, a free space wavelength  $\lambda_0 = 1$  m and the z and x axis ranges are fixed to  $4\lambda_0$ . All the magnetic fields are multiplied by the impedance of medium 1,  $\eta_1$ , to have all the values in the same range for a convenient pseudo-color graph with a color code around the black color. The graphs are time animated by depicting successively several snapshots within one period.

## 5.2. A few exercises

The first exercise is made with  $\varepsilon_{r1} = 1$  and  $\varepsilon_{r2} = 4$  and normal incidence ( $\theta_i = 0^\circ$ ) for perpendicular polarization. **Figure 13** depicts some results shown for this case. Check the reflection and transmission coefficients (similar to a transmission line terminated by a resistive load). Verify

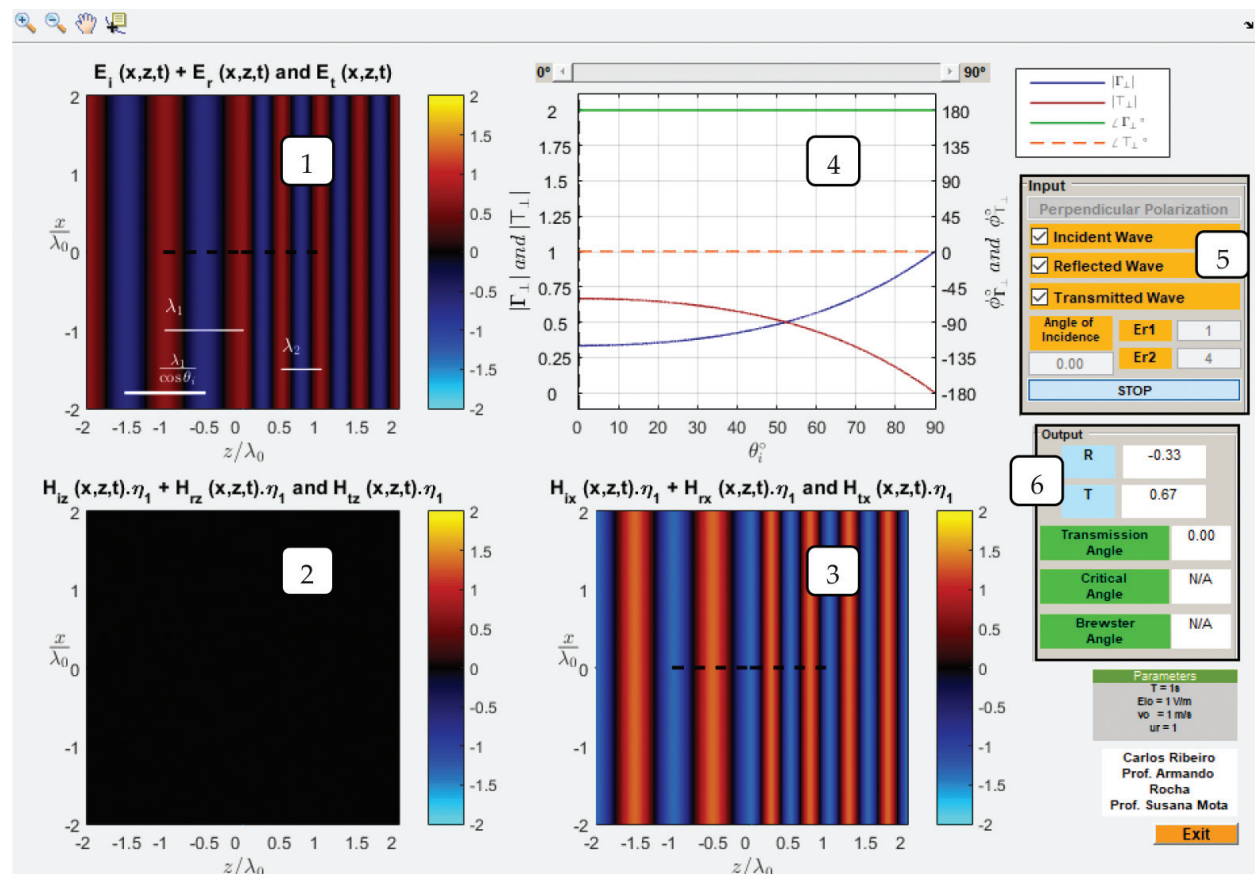


**Figure 13.** EM.m tool screen shot: frame description is given below.



that they are the same for the parallel polarization and also that  $\Gamma_{\perp}$  increases monotonically from  $\theta_i = 0^\circ$  to  $90^\circ$  up to 1 (text frame (3)).

Observe the incident, the reflected and total fields and the standing waves in medium 1. The minima (black stripes) and the maxima (more hot colors and cold colors) occur always at planes parallel to the reflection plane, in spite of a travel in time being observed (left side of text frames (1): electric field  $E_y$  and (3): magnetic field  $H_x$ ). Also the distance between maxima and minima is a quarter of the wavelength. In medium 2 the wave is traveling to the right and has half of the wavelength of that in medium 1, due to the higher dielectric constant (right side of text frames (1) and (3)). No interference is observed because only one traveling wave exists. The component of the magnetic field (text frame (2)) along z-axis does not exist for this particular geometry as can be confirmed by checking **Figure 12**.

The dielectric constant for medium 2 can be increased to observe a larger standing wave amplitude (on the limit an infinite dielectric constant mimics a perfectly conducting medium). There is no perceived advance in medium 2 and the standing wave is depicted as flashing stripes alternating between a light blue and yellow colors. The physical situation is similar to an ideal resonant circuit where energy is being transferred between the inductor (magnetic field) and the capacitor (electric field) with no dissipated power (transmitted).

The second exercise uses the same configuration but considering  $\theta_i = 45^\circ$  and the results are presented in **Figure 14**. Observe the interference in medium 1: the distances of the maxima and minima are now longer and the interference is more “intense”, due to a higher amplitude of the reflected wave. There is a perception of the wave in medium 1 traveling along x and the interference occurring along  $z^-$ . The wave in medium 2 moves away along the direction  $\theta_t$ .

The third exercise ( $\epsilon_{r1} = 1$  and  $\epsilon_{r2} = 4$ ) uses parallel polarization and incidence with the Brewster angle,  $\theta_i = 63.43^\circ$  (Eq. (7)) and the results are depicted in **Figure 15**. The reflection coefficient is null and, as in other cases, increases again up to 1 for tangential incidence after changing sign at the Brewster angle. By observing the total field, check that there is no reflected wave and consequently no interference in medium 1. This means that all the incident power at this polarization and angle of incidence is entirely transmitted to medium 2: an incident circular polarization would give a reflected wave with linear polarization. In addition, it is

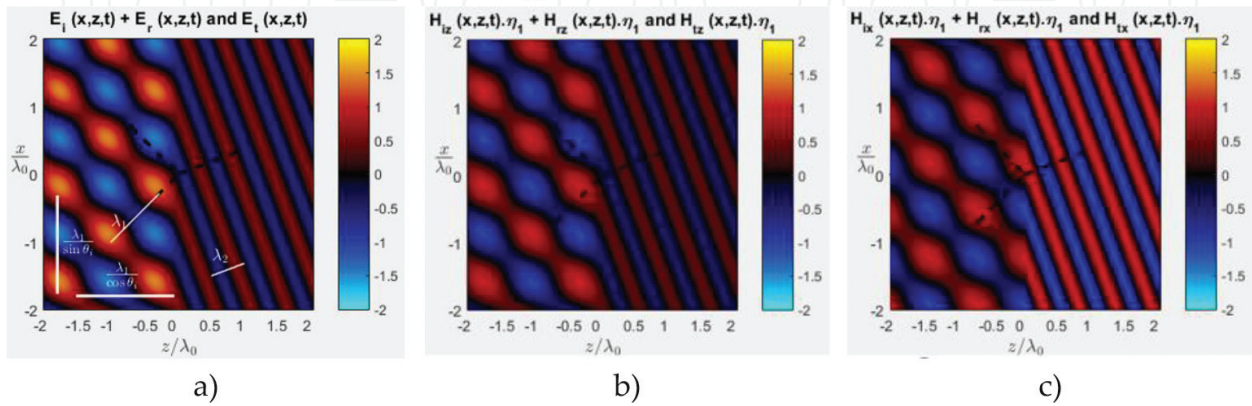


**Figure 14.** Incidence:  $\theta_i = 45^\circ$  (a) electric field  $E_y$  (b) magnetic field  $H_z$  and (c) magnetic field  $H_x$ .

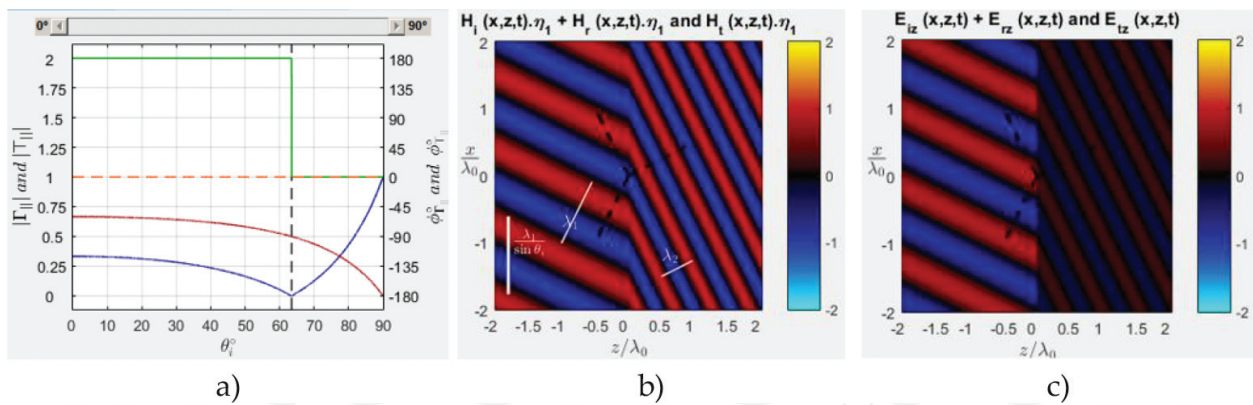


**Figure 15.** (a)  $\Gamma_{||}$  and  $T_{||}$  (b) magnetic field  $H_y$  and (c) electric field  $E_z$ .

interesting to observe the discontinuity of the electric field,  $E_z$ , at the interface between the two mediums (see **Figure 15(c)**), as it is expected from the boundary conditions. It is worthwhile to verify that the Brewster angle does not exist for the perpendicular polarization.

The fourth exercise ( $\epsilon_{r1} = 4$  and  $\epsilon_{r2} = 1$ ) uses parallel polarization and illustrates the incidence above the critical angle  $\theta_{ic} = 30^\circ$  (Eq. (8)). Start by an angle of incidence a few degrees below  $\theta_{ic}$  and check that the angle of transmission is close to  $90^\circ$ . Increasing the angle of incidence a few degrees past  $\theta_{ic}$  allows to observe the results of **Figure 16**: the reflection coefficient becomes real and unitary (full reflection) at  $\theta_{ic}$  and complex (but unitary) at higher angles.

The fields inside medium 2 assume a tooth-like shape along the  $z$ -axis, the amplitude decreases with the distance  $z$  from the reflection plane and the wave travels along  $x$ . By increasing angle of incidence, the fields become closer to the reflection plane. That is, there is no power transferred to medium 2 and the wave is contained in medium 1 by a dielectric based “container”. The angle  $\theta_t$  becomes complex, Eq. (4), and an attenuation constant emerges from the exponentials in Eqs. (13), (14), (19) and (20).

Check that the phenomena occurs for both parallel and perpendicular polarization and only when medium 1 is more “dense” ( $\epsilon_{r1} < \epsilon_{r2}$ ).

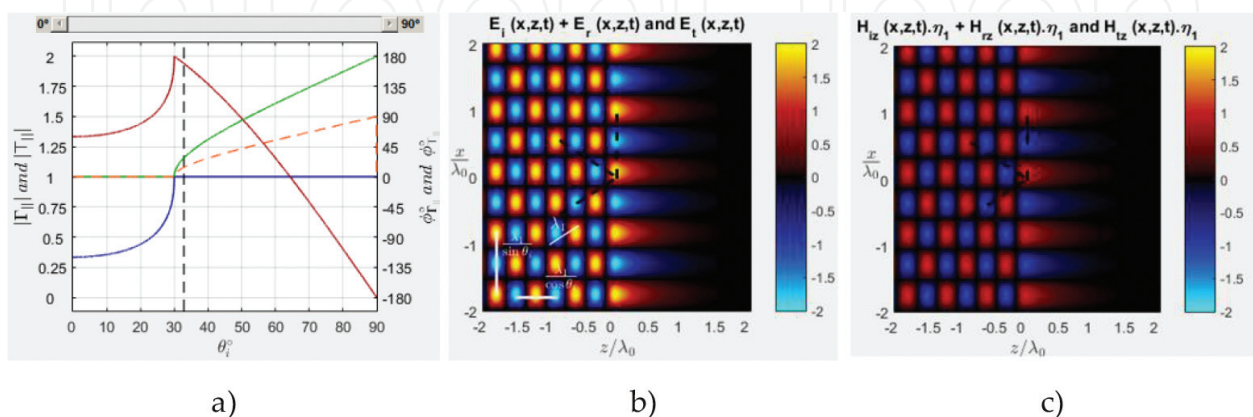


**Figure 16.** Incidence above  $\theta_{ic}$ : (a)  $\Gamma_{\perp}$  and  $T_{\perp}$  (b) electric field  $E_y$  and (c) magnetic field  $H_z$ .

## 6. Conclusions

Simulation tools, to explore the basic concepts about transmission line propagation and about reflection and transmission of plane waves, were described. Moreover, some theoretical exercises were given and, in addition, a few laboratory prototypes measurements depicting the theoretical exercises were presented, thus, highlighting the usefulness of the tools, as well as, the need to complement the learning by using simulations with practical laboratory experiences.

## Acknowledgements

The authors are grateful to the Department of Electronics, Telecommunications and Informatics for the opportunity of teaching this subjects and using the RF equipment to perform the laboratory measurements. They are also grateful to the former MSc student, C. Ribeiro, for the intense brainstorming with them and for the implementation of the simulation tools.

## Author details

Susana Mota\* and Armando Rocha

\*Address all correspondence to: smota@ua.pt

Departamento de Eletrónica, Telecomunicações e Informática, Instituto de Telecomunicações, Aveiro, Portugal

## References

- [1] Rocha A, Mota S, Ribeiro C. Software tools for teaching wave propagation in transmission lines [education corner]. IEEE Antennas and Propagation Magazine. 2017;59(3):118-127
- [2] Trintinalia LC. Simulation tool for the visualization of EM wave reflection and refraction. IEEE Antennas and Propagation Magazine. 2013;55(1):203-211